RSC Advances

PAPER

View Article Online
View Journal | View Issue

Cite this: *RSC Adv.*, 2020, **10**, 15881

Organic–inorganic hybrid coating materials derived from renewable soybean oil and amino silanes†

Xuyang Luo, Fei Gao,* Fengbiao Chen, Qian Cheng, Jinze Zhao, Xiao Wei, Cong Lin, Jiang Zhong and Liang Shen*

Received 10th February 2020
Accepted 15th April 2020

DOI: 10.1039/d0ra01279c

rsc.li/rsc-advances

Novel organic–inorganic hybrid coating materials were developed using amino silanes and acetoacetylated soybean oil. The acetoacetylated soybean oil was prepared from soybean oil (a renewable resource) using a solvent-free method involving a thiol–ene and transesterification reactions, and the chemical structure was characterized by nuclear magnetic resonance (NMR), gel permeation chromatography (GPC), Fourier-transform infrared (FTIR) spectroscopy, and viscosity analyses. On the basis of the acetoacetylated soybean oil, several organic–inorganic hybrid coating materials were prepared using different amino silanes by a catalyst-free method involving one-step comprising two reactions (an amine–acetoacetate reaction and an *in situ* sol–gel technique), and their crosslinked structures were determined from their FT-IR and solid-state ^{29}Si NMR spectra. The resulting coating materials have good mechanical/chemical performance. This method for preparing renewable organic–inorganic hybrid coating materials may have wide uses because plant oils contain many unsaturated C=C bonds and easy access to acetoacetate functional groups.

Introduction

In recent years, the use of renewable resources to replace petroleum as a raw material in the preparation of coating materials has received considerable attention because of the demands placed on fossil feedstocks and environmental issues.[1–4] Vegetable oils, as renewable resources, have unique chemical structures containing hydroxyls, esters, unsaturated sites, and other functional groups, and these can be modified to make low molecular weight polymeric materials for a range of versatile applications.[5–9]

Acetoacetyl chemistry is interesting to use to prepare thermoset resins because acetoacetate functional groups can react with various groups,[10–13] including aldehydes,[14] isocyanates,[15] acrylates,[16] and amines.[17] Although many thermoset resins have been prepared using acetoacetate chemistry and amines, only a few studies have been reported on the synthesis of biobased coating materials. Trumbo and co-workers[18] developed novel biobased coating materials from multifunctional amines and acetoacetylated castor oil, and the properties of the coatings were found to be improved by increasing the temperature. Webster and co-workers[19] invented novel biobased coating materials based on multifunctional amines and acetoacetylated sucrose, and the properties of the obtained coatings could be enhanced by adjusting the degree of substitution in the acetoacetylated sucrose. Recently, our group[20] has reported biobased coating materials that were developed using modified acetoacetylated castor oil and multifunctional amines, and their properties were found to be improved upon increasing the acetoacetate group content. However, the preparation of organic–inorganic hybrid coating materials from acetoacetylated plant-based materials has not yet been reported.

Recently, we have been interested in the synthesis of organic–inorganic hybrid materials because of their novel chemical and physical properties.[21,22] Silica-based hybrids are promising for use in the preparation of organic–inorganic hybrid materials, in which the condensation of organosiloxane precursors can be carried out a *via* sol–gel technique, and these materials are useful in many fields of technology, including electronic materials,[23] separation science,[24] solid electrolytes,[25] as functional coatings,[26] and so on.

In this work, we develop a novel organic–inorganic hybrid coating material based on acetoacetylated soybean oil, the reaction mechanism of which is shown in Scheme 1. The primary novelties of this study include: (1) acetoacetylated soybean oil is prepared from soybean oil *via* a solvent-free method, (2) organic–inorganic hybrids coating materials can be obtained in one step comprising two reactions (amine–acetoacetate reaction and *in situ* sol–gel technique), and (3) the method presented here is excellent for preparing renewable

Jiangxi Engineering Laboratory of Waterborne Coating, School of Chemistry and Chemical Engineering, Jiangxi Science & Technology Normal University, Nanchang 330013, Jiangxi, P. R. China. E-mail: feigao2016@jxstnu.com.cn; liangshen@jxstnu.com.cn

† Electronic supplementary information (ESI) available. See DOI: 10.1039/d0ra01279c

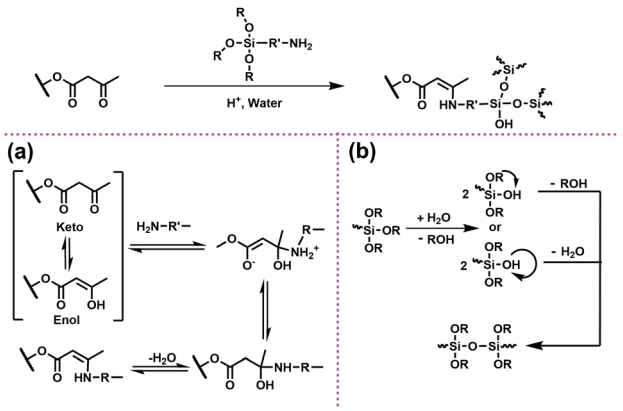

Scheme 1 The reaction mechanism of the preparation of organic–inorganic hybrid coating materials *via* (a) an amine–acetoacetate reaction and (b) an *in situ* sol–gel technique.

organic–inorganic hybrid coating materials because plant oils contain many unsaturated C=C bonds and provide easy access to acetoacetate functional groups.

Experimental

Materials

Soybean oil (SO), 2-mercaptoethanol, 2-hydroxy-2-methylpropheone (1173), and *p*-toluenesulfonic acid were purchased from Tianjin Biochemical Technology Co., Ltd, China. (3-Aminopropyl) trimethoxysilane (**B1**), (3-aminopropyl)triethoxysilane (**B2**), -*N*-[3-(trimethoxysilyl)propyl]ethylenediamine (**B3**), and *t*-butyl acetoacetate were purchased from Shanghai Aladdin Biochemical Technology Co., Ltd, China. Solvents such as tetrahydrofuran (THF), absolute ethanol, and acetone were purchased from Adamas Reagent, Ltd. All of the above-mentioned chemicals were used without any further purification. The water (H_2O) used in this was deionized and doubly distilled.

Preparation of the modified soybean oil

The method for preparing the modified soybean oil is shown in Scheme 2 and was carried out as follows. A solution of soybean oil (8.95 g, 10 mmol, 1 eq.) and 2-hydroxy-2-methylpropio phenone (equal to 5 wt% of the total weight) in a reaction bottle was stirred under nitrogen for 10 min. Then, 2-mercaptoethanol (4.7 g, 60 mmol, 6 eq.) was added, and the mixture was stirred for another 3 min. The reaction was then stimulated by ultraviolet light (8 mW, 365 nm) for 5.5 h. After reaction, the excess 2-mercaptoethanol in the product was removed by vacuum distillation at 110 °C and a yellow oil (**A2**) was obtained in a yield of 98% (calculated by ^{1}H NMR, see Fig. S1†).^{1}H NMR ($CDCl_3$, 400 MHz): δ (ppm) = 5.27 (s, 1H), 4.76–4.65 (m, 4H), 4.33–4.08 (m, 4H), 3.97–3.62 (m, 10H), 2.95–2.51 (m, 10H), 2.39–2.21 (m, 5H), 2.05–1.48 (m, 54H), 1.48–1.02 (m, 54H), 0.96–0.77 (m, 9H). ^{13}C NMR ($CDCl_3$, 400 MHz): δ (ppm) = 174.90, 174.45, 79.16, 78.85, 78.58, 70.45, 63.61, 62.72, 61.84, 47.41, 47.29, 45.05, 44.86, 42.79, 45.05, 44.86, 42.79, 37.91, 36.59, 36.44, 35.65, 35.51, 34.96, 34.61, 33.41, 33.29, 33.17, 32.98, 31.13, 30.80, 30.52, 28.27, 28.05, 26.32, 24.16, 15.65. GPC (theoretical formula weight = 1272 g mol^{-1}); M_n = 1243 g mol^{-1}, M_w = 1528 g mol^{-1}, dispersity ($Đ$) = 1.2. Viscosity: 6.5 Pa s.

Preparation of acetoacetylated soybean oil

The method for preparing acetoacetylated soybean oil is shown in Scheme 3 and was carried out as follows. A 100 mL round-bottomed flask equipped with a magnetic stirrer bar under nitrogen was loaded with modified soybean oil (**A2**) (12.72 g, 10 mmol, 1 eq.) and *t*-butyl acetoacetate (7.91 g, 50 mmol, 5 eq.). The reaction mixture was stirred at 110 °C for 10 h and the liquid of *t*-butanol was removed with distillation, after which the excess *t*-butyl acetoacetate was removed by vacuum distillation at 140 °C. Finally, a yellow oil (**A3**) was obtained in a yield of 93% (calculated by ^{1}H NMR, see Fig. S2†). ^{1}H NMR ($CDCl_3$, 400 MHz): δ (ppm) = 5.25 (s, 1H), 4.46–4.29 (m, 10H), 4.29–4.08 (m, 4H), 3.53–3.42 (m, 10H), 3.02–2.88 (m, 10H), 2.83–2.52 (m, 11H), 2.37–2.19 (m, 15H), 1.79–1.45 (m, 13H), 1.45–1.05 (m, 54H), 0.94–0.78 (m, 9H). ^{13}C NMR ($CDCl_3$, 400 MHz): δ (ppm) = 201.39, 174.15, 168.29, 90.94, 79.30, 78.98, 78.71, 70.37, 65.93, 64.85, 64.31, 63.50, 61.37, 47.66, 45.63, 38.47, 37.60, 36.30, 35.51, 33.28, 30.81, 28.15, 26.30, 24.14, 15.55. GPC (theoretical formula weight = 1693 g mol^{-1}); M_n = 1676 g mol^{-1}, M_w = 2045 g mol^{-1}, dispersity ($Đ$) = 1.2. Viscosity: 2.3 Pa s.

Preparation of the organic–inorganic hybrid coating material

The methods used to prepare the films are shown in Scheme 4 and Table 1, and were carried out as follows. Acetoacetylated soybean oil (0.591 mmol) and cross-linker (2.96 mmol) were dissolved in 3 mL of THF (1 : 1 ratio based on the functional groups) and allowed to mix for 5 min. Then, water (1.5 mL) and ethanol (2 mL) were added to the system, which was mixed. The mixture was poured into a poly(tetrafluoroethylene) (PTFE) mold (8 × 8 × 1.5 cm), and finally, the films were cured *via* an amine–acetoacetate reaction and hydrolyzed *in situ* for 3 h at 30 °C, followed by 5 h at 80 °C, to give a dry film (350–450 micron thickness). In order to ensure full solvent removal, the films were further placed in a vacuum oven for 36 h at 60 °C.

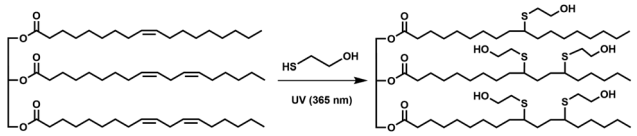

Scheme 2 The synthesis of modified soybean oil.

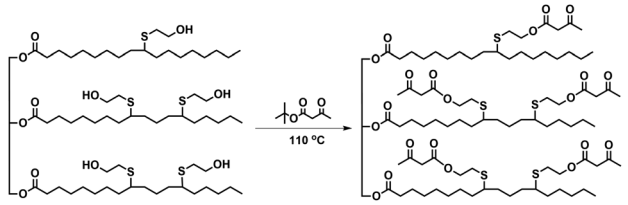

Scheme 3 The synthesis of acetoacetylated soybean oil.

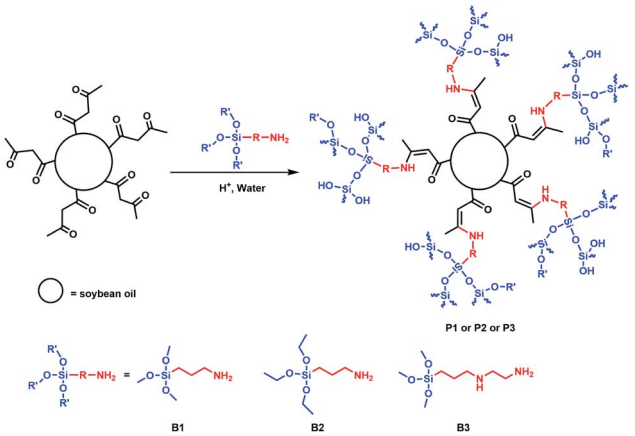

Scheme 4 Synthetic route of the organic–inorganic hybrid coating materials.

Table 1 Film codes and compositions of the organic–inorganic hybrid coating materials prepared in this study

Sample code	Acetoacetylated soybean oil (mmol)	Cross-linker (mmol)	Acetoacetate/amine ratio
P1	0.591	2.96 (**B1**)	1 : 1
P2	0.591	2.96 (**B2**)	1 : 1
P3	0.591	2.96 (**B3**)	1 : 1

Characterization

FTIR spectra were recorded using a Bruker Vertex70 spectrometer in attenuated total reflection (ATR) mode using an average of 32 scans for each sample over the range of 4000–500 cm^{-1}, with a resolution of 4 cm^{-1} at room temperature.

^{1}H and ^{13}C NMR spectra were collected using a Bruker AV-400 NMR instrument, where tetramethylsilane (TMS) was used as an internal reference and deuterated chloroform ($CDCl_3$) was used as a solvent. Solid-state ^{29}Si NMR spectra were collected using a Fourier-transform Bruker 600 MHz wide bore solid spectrometer (model Avance III HD).

Thermogravimetric analysis (TGA) was performed using a TGA-Q50 system obtained from TA Instruments and the measurements were carried out from room temperature to 750 °C at a heating rate of 10 °C min^{-1} under a N_2 atmosphere.

Dynamic mechanical analysis (DMA) of the films was performed using a (TA Instruments Q800, New Castle, De) dynamic mechanical analyzer with a film tension mode of 1 Hz. The samples were cooled in liquid nitrogen and held isothermally at −80 °C for 3 min, and then heated to 100 °C at a rate of 5 °C min^{-1}. The storage moduli, loss moduli, and tan δ of the films were studied under a controlled temperature.

The DSC experiments were performed on a TA calorimeter (TA-Q200, TA). The polymer sample was heated at a rate of 10 °C min^{-1} from −40–200 °C at a rate of 10 °C min^{-1} under a nitrogen atmosphere and heat capacity data of the samples were collected during the second heating process.

Gel permeation chromatography (GPC) was performed on a GPC apparatus (Waters 515; Waters, USA) at 25 °C. The samples were diluted to 2 mg mL^{-1} in THF for the GPC runs, where THF was used as an eluent at a flow rate of 1.0 mL min^{-1}, and the molecular weights were determined using polystyrene standards.

A TA Discovery HR-2 Rheometer was used to measure the viscosity of the soybean oil (**A1**), modified soybean oil (**A2**), and modified acetoacetylated soybean oil (**A3**).

The gel content was determined by immersion of a film (2 × 2 cm piece) with a known weight (W_1). The dried film was immersed in acetone for 48 h and then dehydrated for 48 h at 60 °C to provide a weight, W_2. The gel content M (%) was then calculated according to the following formula: M (%) = W_2/W_1 × 100%.

Results and discussion

Characterization of acetoacetylated soybean oil

In this study, the soybean oil used contains five C=C bonds per molecule, as confirmed by ^{1}H NMR spectroscopy (Fig. S1a, ESI†). The chemical structure of the obtained acetoacetylated soybean oil was also confirmed by NMR, GPC, and FTIR spectroscopy. As shown in Fig. 1a, the peaks (soybean oil, **A1**) at 5.26 and 5.53 ppm ((c and d), correspond to the C=C bonds of the soybean oil) disappeared after the thiol–ene coupling reaction, and new peaks appeared at 3.68 and 3.85 ppm (e and f), which can be attributed to methyl carbons (grafting of 2-mercaptoethanol in the modified soybean oil (**A2**), by approximately 98%, Fig. S1b, ESI†). Compared to the acetoacetylated soybean oil (**A3**) and modified soybean oil (**A2**), the peaks at 3.68 and 3.85 ppm (e and f) shifted to 4.33–4.45 ppm (i) and the new peaks of the acetoacetyl group appeared at 3.5 ppm (g) and 2.36 ppm (h) (by approximately 93%, Fig. S2, ESI†). The ^{13}C NMR spectra of the acetoacetylated soybean oil are shown in Fig. 1b. The intensities of the C=C bond peaks of the soybean

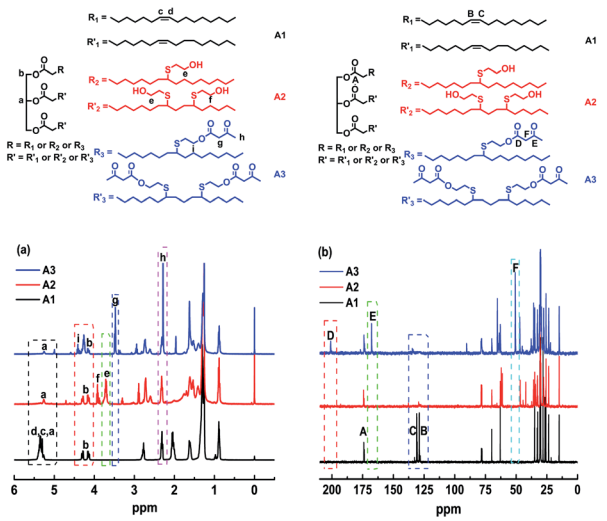

Fig. 1 (a) ^{1}H and (b) ^{13}C NMR spectra of the acetoacetylated soybean oil.

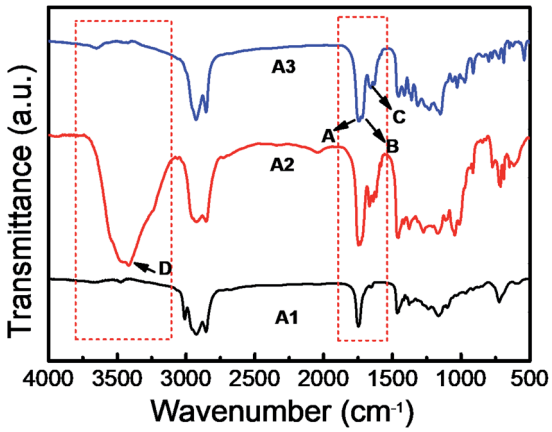

Fig. 2 FTIR spectra of the soybean oil (A1), modified soybean oil (A2), and acetoacetylated soybean oil (A3).

oil (**A1**) at 126 ppm (B) and 130 ppm (C) decreased after the thiol–ene coupling reaction and new peaks for the acetoacetylated soybean oil (**A3**) appeared at 201 ppm (D) and 170 ppm (E). In addition, compared with the GPC curves of the soybean oil (**A1**), modified soybean oil (**A2**), and acetoacetylated soybean oil (**A3**) (Fig. S3, ESI†), the number average molecular weight was increased after the thiol–ene coupling reaction and transesterification reactions. These results show that acetoacetylated soybean oil was obtained.

The FTIR spectra of the acetoacetylated soybean oil are shown in Fig. 2. Comparing the spectrum of the soybean oil (**A1**) to that of the modified soybean oil (**A2**), new peak appears at 3430 cm^{-1} (D), corresponding to the absorption peak of the OH group, which indicates that the soybean oil reacted with 2-mercaptoethanol to gain OH groups. Comparing the modified soybean oil (**A2**) and acetoacetylated soybean oil (**A3**), the absorption band at 3430 cm^{-1} (D) in the acetoacetylated soybean oil (**A3**) disappeared and new peaks (acetoacetyl groups) appeared at 1740 cm^{-1} (B) and 1650 cm^{-1} (C). These results further confirmed that the acetoacetylated soybean oil was obtained.

Fig. 3 shows the viscosities of soybean oil (**A1**), modified soybean oil (**A2**), and acetoacetylated soybean oil (**A3**). After the thiol–ene coupling reaction, the viscosity increased from 0.05 Pa s (soybean oil) to 6.5 Pa s (modified soybean oil) because of the increase in the number of intermolecular hydrogen bonds.[27] However, after the transesterification reaction from modified soybean oil to acetoacetylated soybean oil, the viscosity decreased to 2.3 Pa s. The main reason for this was that the hydrogen bonding interactions were weakened by the transesterification reaction.

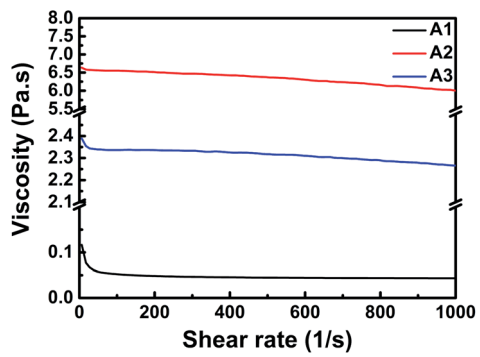

Fig. 3 Rheological viscosity *versus* the shear rate for soybean oil (A1), modified soybean oil (A2), and acetoacetylated soybean oil (A3).

Characterization of the films

In order to explore the properties of the organic–inorganic hybrid coating materials, three films (**P1**, **P2**, and **P3**) were prepared *via* an amine–acetoacetate reaction and the sol–gel technique, in which the acetoacetylated soybean oil was reacted with different crosslinkers (**B1**, **B2** or **B3**) at a molar ratio of acetoacetate to amino-groups of 1 : 1 (for full experimental details see the Experimental section). The structures of the dried organic–inorganic hybrid coatings were determined by FTIR and solid-state ^{29}Si NMR analyses. As shown in Fig. 4, the structures of the films (**P1**, **P2**, and **P3**), acetoacetylated soybean oil (**A3**), and crosslinkers (**B1**, **B2**, and **B3**) were confirmed from their FTIR spectra. The C=O stretching peaks (acetoacetylated soybean oil) at 1730 and 1650 cm^{-1} disappeared, and new peaks at 1640 cm^{-1} (C=O), 1605 cm^{-1} (C=C), and 3346 cm^{-1} (N–H) were observed in the three films. The absorption peaks at 1100 cm^{-1} (Si–O–Si asymmetric stretching), 1120 cm^{-1} (Si–O–Si symmetric stretching), 800 cm^{-1} (symmetrical Si–O–Si stretching), and 3400–3500 cm^{-1} (Si–OH groups) clearly demonstrate the success of using the sol–gel technique.[28]

The solid-state ^{29}Si NMR of the three films (**P1**, **P2**, and **P3**) are shown in Fig. 5, which confirm the formation of the Si–O–Si bonds and network structure. In the spectra, only two peaks can be observed, and the peak at −68.46 ppm (T^3 structure) is more obvious than the other peak (T^2, −59.40 ppm), and the peak at −49.98 ppm (T^1 structure) is almost absent.[29] These results

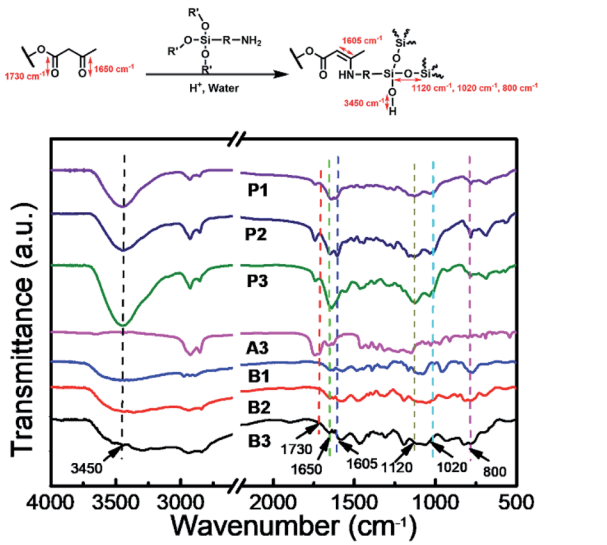

Fig. 4 FTIR spectra of the three films (P1, P2, and P3), acetoacetylated soybean oil (A3), and the crosslinkers (B1, B2, and B3).

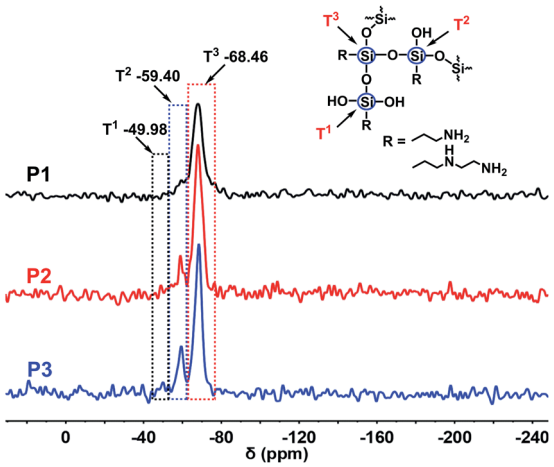

Fig. 5 The solid-state ^{29}Si NMR spectra of the three films (P1, P2, and P3).

indicate that most of the network structure features one Si atom associated with three –Si–O–Si– linkages (T^3), some of the network structure features one Si atom associated with two –Si–O–Si– linkages (T^2), and a network structure with one Si atom associated with one –Si–O–Si– linkage (T^1) is hardly observed. Due to the degree of branching (DB) being an important parameter used to describe the degree of similarity between the branched structure of hyperbranched polymers and ordinary dendritic polymers, it is usually determined from the integral area of the ^{29}Si NMR spectrum according to Frey's equation: $DB = 2D/(2D + L)$.[30,31] Therefore, the DB values of the films were estimated to be 0.95, 0.93, and 0.88, all of which are close to 1, values that are obviously higher than those of traditional hyperbranched polymers. Thus, all three of the films may have a "completely branched" structure.[32]

Gel content

The gel content is a very important parameter that is closely related to the crosslinking density of resins. The gel contents of the three films (**P1**, **P2**, and **P3**) are shown in Table 2, where it can be seen that the films have a high gel content (higher than 97%). The results show that the three films undergo high chemical reaction and have a high crosslinking density.

Mechanical properties

Fig. 6 shows the storage moduli and loss factor (tan δ) dependent on the temperature for the three films (**P1**, **P2**, and **P3**) with

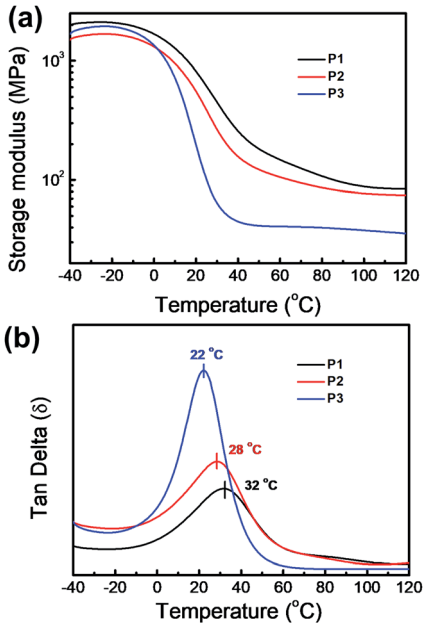

Fig. 6 Dynamic mechanical analysis (DMA) of the three films (P1, P2, and P3): (a) storage modulus and (b) loss factor (tan δ) as a function of the temperature of the three films.

different crosslinkers (**B1**, **B2**, and **B3**). The storage moduli (E') of all of the films showed a similar trend with a change in temperature (Fig. 6a); with an increase in the temperature, the storage modulus (E') decreased rapidly and finally stabilized. The loss factors (tan δ) of these films are shown in Fig. 6b. Only one peak was observed in each case, indicating that the three films exhibit homogeneous properties. The glass transition temperature (T_g) was obtained according to the peak maximum value.

The crosslink density was the calculated using the following formula:[32–34]

$$ve = E'/3RT$$

where E' is the storage modulus of the thermoset polymer in the rubbery plateau region at T_g + 50 °C, R is the universal gas constant, and T is the absolute temperature. The glass transition temperature (T_g), tan δ, and crosslinking density (ve) values of the three films are summarized in Table 2. Comparing the three films, **P1** has the highest glass transition temperature (T_g)

Table 2 Summary of gel contents and DMA dates and thermal properties of the three films (P1, P2, and P3)[a]

Sample code	Gel content (%)	Young's modulus (MPa)	Stress at break (MPa)	Elongation at break (%)	tan δ	T_g (at tan δ) (°C)	E' at T_g + 50 °C (MPa)	Crosslink density (ve) (mol m^{-3})	TGA in nitrogen (°C)				DSC T_g (°C)
									T_5	T_{10}	T_{50}	T_{max}	
P1	98	486 ± 24	3.74 ± 0.51	1.16 ± 0.05	0.24	32	104	11 785	254	303	465	605	27
P2	97	97 ± 5	2.89 ± 0.23	4.31 ± 0.24	0.32	28	87	9965	251	295	462	601	22
P3	97	8 ± 0.5	0.43 ± 0.02	6.61 ± 0.41	0.57	22	41	4686	204	258	428	581	12

[a] T_5, T_{10}, T_{50}, and T_{max} represent the temperatures at which the mass loss is 5, 10, and 50 wt%, and the maximum mass loss temperature, respectively.

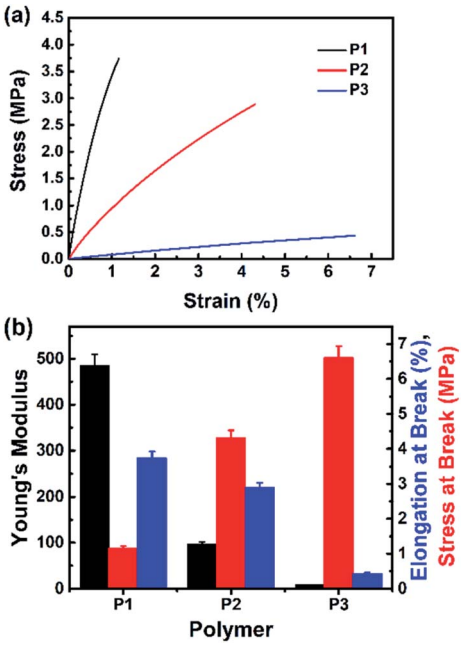

Fig. 7 Stress–strain curves of the three films.

and crosslinking density. The main reason for this may be that the crosslinker C1 has a lower steric hindrance structure.

Fig. 7 presents the stress–strain curves of the films (**P1**, **P2**, and **P3**), and their tensile data (tensile strength, elongation at break, and Young's modulus) are shown in Table 2. Comparing the three films, it is obvious that **P1** has the highest tensile strength and Young's modulus, but the lowest elongation at break value, and **P3** has the lowest tensile strength and Young's modulus, but the highest elongation at break value, which may be because as the crosslinking density decreases, the mechanical properties (tensile strength and Young's modulus) gradually decrease.[35]

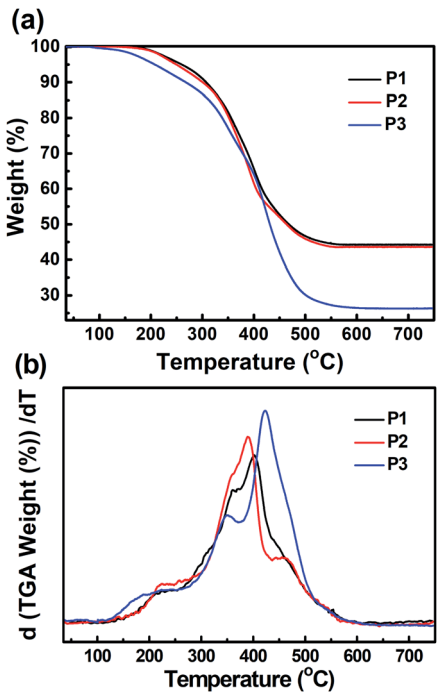

Fig. 8 (a) The TGA and (b) DTGA curves of the three films.

Thermal stability

Fig. 8 shows the TGA and DTGA curves of the three films, and the T_5, T_{10}, T_{50}, and T_{max} data are summarized in Table 2. From Fig. 8a, it can be seen that the TGA curves show a similar trend and two distinct degradation stages are observed for all of the films. The first phase degradation in the range of 180–300 °C can be attributed to the disassociation of unstable ester groups and sulfur–carbon bonds.[36] At the second phase, the temperature in the range of 300–550 °C is related to the scission of the polymer chain.[37] All of the films are stable over 550 °C, but they leave a partial residue, which may be due to the silica from the gas phase oxidation randomly falling on the sample pan or on the weighting arm of the balance.[38] In addition, the T_g values from DSC (details can be found in Fig. S4†) are also presented in Table 2. As can be seen, the T_g values (DSC) are in the order of **P1** > **P2** > **P3**, because as the crosslinking density decreases, the T_g values gradually decrease.

Conclusions

In this paper, a novel organic–inorganic hybrid coating material was synthesized by a one-step comprising two reactions (using amine–acetoacetate reaction and *in situ* sol–gel technique) between amino silanes and acetoacetylated soybean oil. The acetoacetylated soybean oil was obtained from renewable soybean oil using a thiol–ene and transesterification reaction and characterized by NMR, GPC, FTIR, and viscosity analyses. Then, three organic–inorganic hybrid coating materials were prepared by acetoacetylated soybean oil and different amino silanes and their crosslinked structures were determined by FT-IR and solid-state ^{29}Si NMR spectra. The mechanical and thermal properties of these films were characterized by DMA, DSC, and TGA, and the coating materials were found to have good mechanical/chemical properties. The characteristics of this novel system demonstrate the applicability of the organic–inorganic hybrid coating for vegetable oils as a new eco-friendly raw material.

Conflicts of interest

There are no conflicts to declare.

Acknowledgements

This research was funded by the Program for the NSFC of China (No. 51963010, 21704036), Science Funds of the Education Office of Jiangxi Province (No. GJJ170658), the Science Funds of Jiangxi Province (No. 20171BAB216019, No. 20181BAB206016), the Youth Top Talent Support Program of JXSTNU (No. 2019QNBJRC007), and National Training Program of

Innovation and Entrepreneurship for Undergraduates (No. 201911318021).

Notes and references

1 P. B. V. Scholten, C. Detrembleur and M. A. R. Meier, *ACS Sustainable Chem. Eng.*, 2019, **7**, 2751–2762.
2 R. Tramontina, J. L. Galman, F. Parmeggiani, S. R. Derrington, T. D. H. Bugg, N. J. Turner, F. M. Squina and N. Dixon, *Green Chem.*, 2020, **22**, 144–152.
3 E. Kolanthai, K. Sarkar, S. R. K. Meka, G. Madras and K. Chatterjee, *ACS Sustainable Chem. Eng.*, 2015, **3**, 880–891.
4 S. Iravani and R. S. Varma, *Green Chem.*, 2019, **21**, 4839–4867.
5 C. Zhang, S. A. Madbouly and M. R. Kessler, *ACS Appl. Mater. Interfaces*, 2015, **7**, 1226–1233.
6 Z. Liu, J. Chen, G. Knothe, X. Nie and J. Jiang, *ACS Sustainable Chem. Eng.*, 2016, **4**, 901–906.
7 M. Desroches, S. Caillol, V. Lapinte, R. Auvergne and B. Boutevin, *Macromolecules*, 2011, **44**, 2489–2500.
8 D. Guzman, X. Ramis, X. Fernandez-Francos, S. De la Flor and A. Serra, *Prog. Org. Coat.*, 2018, **114**, 259–267.
9 J. Chen, M. de Liedekerke Beaufort, L. Gyurik, J. Dorresteijn, M. Otte and R. J. M. Klein Gebbink, *Green Chem.*, 2019, **21**, 2436–2447.
10 D. Xu, Z. Cao, T. Wang, J. Zhong, J. Zhao, F. Gao, X. Luo, Z. Fang, J. Cao, S. Xu and L. Shen, *Prog. Org. Coat.*, 2019, **135**, 510–516.
11 Z. Cao, F. Gao, J. Zhao, X. Wei, Q. Cheng, J. Zhong, C. Lin, J. Shu, C. Fu and L. Shen, *Polymers*, 2019, **11**, 1809.
12 M. B. Sims, J. J. Lessard, L. Bai and B. S. Sumerlin, *Macromolecules*, 2018, **51**, 6380–6386.
13 T. Wright, T. Tomkovic, S. G. Hatzikiriakos and M. O. Wolf, *Macromolecules*, 2018, **52**, 36–42.
14 X. He, J. Zhong, Z. Cao, J. Wang, F. Gao, D. Xu and L. Shen, *Prog. Org. Coat.*, 2019, **129**, 21–25.
15 Z. Liu, C. Yu, C. Zhang, Z. Shi and J. Yin, *ACS Macro Lett.*, 2019, **8**, 233–238.
16 T. Wang, J. Wang, X. He, Z. Cao, D. Xu, F. Gao, J. Zhong and L. Shen, *Coatings*, 2019, **9**, 37.
17 W. Denissen, M. Droesbeke, R. Nicolaÿ, L. Leibler, J. M. Winne and F. E. D. Prez, *Nat. Commun.*, 2017, **8**, 14857.
18 A. S. Trevino and D. L. Trumbo, *Prog. Org. Coat.*, 2002, **44**, 49–54.
19 P. Xiao, T. J. Nelson and D. C. Webster, *Prog. Org. Coat.*, 2012, **73**, 344–354.
20 H. Zuo, Z. Cao, J. Shu, D. Xu, J. Zhong, J. Zhao, T. Wang, Y. Chen, F. Gao and L. Shen, *Prog. Org. Coat.*, 2019, **135**, 27–33.
21 C. Q. Fu, X. Z. Hu, Z. Yang, L. Shen and Z. T. Zheng, *Prog. Org. Coat.*, 2015, **84**, 18–27.
22 C. Q. Fu, Z. Yang, Z. T. Zheng and L. Shen, *Prog. Org. Coat.*, 2014, **77**, 1241–1248.
23 A. Walcarius, *Chem. Mater.*, 2001, **13**, 3351–3372.
24 U. Díaz, Á. Cantín and A. Corma, *Chem. Mater.*, 2007, **19**, 3686–3693.
25 C.-L. Lin, M.-Y. Yeh, C.-H. Chen, S. Sudhakar, S.-J. Luo, Y.-C. Hsu, C.-Y. Huang, K.-C. Ho and T.-Y. Luh, *Chem. Mater.*, 2006, **18**, 4157–4162.
26 K.-M. Jeong, S. S. Park, S. Nagappan, G. Min, Y. Zhang, M. Qu, Y. Zhang and C.-S. Ha, *Prog. Org. Coat.*, 2019, **134**, 323–332.
27 Y. Yin, L. Ma, S. Wen and J. Luo, *J. Phys. Chem. C*, 2018, **122**, 19931–19936.
28 M. A. de Luca, M. Martinelli, M. M. Jacobi, P. L. Becker and M. F. Ferrão, *J. Am. Oil Chem. Soc.*, 2006, **83**, 147–151.
29 C. Zhang, H. Wang, W. Zeng and Q. Zhou, *Ind. Eng. Chem. Res.*, 2019, **58**, 5195–5201.
30 C. J. Hawker, R. Lee and J. M. J. Frechet, *J. Am. Chem. Soc.*, 1991, **113**, 4583–4588.
31 H. Frey, *Acta Polym.*, 1997, **48**, 298–309.
32 X. F. Lei, Y. Chen, H. P. Zhang, X. J. Li, P. Yao and Q. Y. Zhang, *ACS Appl. Mater. Interfaces*, 2013, **5**, 10207–10220.
33 K. K. Jena and K. V. S. N. Raju, *Ind. Eng. Chem. Res.*, 2008, **47**, 9214–9224.
34 H. Ni, A. D. Skaja and M. D. Soucek, *Prog. Org. Coat.*, 2000, **40**, 175–184.
35 D. Xu, Z. Cao, T. Wang, J. Zhao, J. Zhong, P. Xiong, J. Wang, F. Gao and L. Shen, *ACS Omega*, 2019, **4**, 11173–11180.
36 M. Ionescu, D. Radojčić, X. Wan, M. L. Shrestha, Z. S. Petrović and T. A. Upshaw, *Eur. Polym. J.*, 2016, **84**, 736–749.
37 Y. Feng, H. Liang, Z. Yang, T. Yuan, Y. Luo, P. Li, Z. Yang and C. Zhang, *ACS Sustainable Chem. Eng.*, 2017, **5**, 7365–7373.
38 T. Gurunathan and J. S. Chung, *ACS Sustainable Chem. Eng.*, 2016, **4**, 4645–4653.